PERGAMON

Carbon 40 (2002) 2673–2683

CARBON

Surface chemistry of ordered mesoporous carbons

H. Darmstadt[a,*], C. Roy[a], S. Kaliaguine[a], S.J. Choi[b], R. Ryoo[b]

[a]*Chemical Engineering Department, Université Laval, Québec QC, G1K 7P4, Canada*

[b]*National Creative Research Initiative Center for Functional Nanomaterials and Department of Chemistry, School of Molecular Science-BK21, Korea Advanced Institute of Science and Technology, Taejon 305-701, South Korea*

Received 1 November 2001; accepted 15 May 2002

Abstract

Ordered mesoporous carbons (OMC) were produced by pyrolysis of hydrocarbons adsorbed in two different silica matrices (MCM-48 and SBA-15), followed by dissolution of the matrix in either hydrofluoric acid or sodium hydroxide. Some carbons were subsequently heat treated at temperatures of up to 1600 °C. The chemistry of the external surface was studied by X-ray photoelectron spectroscopy (XPS) and static secondary ion mass spectroscopy (SIMS). Information on the graphitic order of the surface of the mesopores was obtained from low-pressure nitrogen adsorption data. The external and internal surface of the OMC has a polyaromatic, graphite-like character. This character increases considerably with increasing pyrolysis and/or post-pyrolysis temperature, as expected. According to the XPS and the nitrogen adsorption data, this increase was especially pronounced for temperatures above 1100 °C. In spite of the different pore structures, only small differences in the polyaromatic character were found for OMC synthesised either in a MCM-48 or in a SBA-15 matrix. Differences exist for the non-carbon elements. When hydrofluoric acid is used for dissolution of the silica matrix, organic fluorine compounds are formed. Their concentration is higher when a MCM-48 matrix as opposed to a SBA-15 matrix was used. Dissolution of the silica matrix in sodium hydroxide yielded a less contaminated OMC as compared to dissolution in hydrofluoric acid.

Keywords: A. Porous carbon; B. Carbonisation; Heat treatment; C. X-ray photoelectron spectroscopy; D. Surface properties

1. Introduction

In a previous investigation, the pore structure of ordered mesoporous carbons (OMC) synthesised in two silica matrices [1,2] was studied by low-pressure nitrogen adsorption [3]. In addition to the pore structure, the surface chemistry is also very important for the adsorption behaviour [4–7]. Therefore, in the present work, the surface chemistry of the OMC was studied in detail by two spectroscopic methods: X-ray photoelectron spectroscopy (XPS) and static secondary ion mass spectroscopy (SIMS). The combination of these two techniques is attractive since different portions of the surface are studied. Static SIMS only probes the first atomic layer, whereas by XPS information on the surface chemistry up to a depth of approximately 50 Å is obtained. Thus, by XPS, in addition to the surface, near-surface regions are also studied.

It should be mentioned that the largest portion of the surface of the OMC is located in mesopores. The outer surface studied by XPS and SIMS represents therefore only a small portion of the total surface. However, it was possible to obtain information on the mesopore surface from low-pressure nitrogen adsorption data [3]. In the sub-monolayer region, the shape of the nitrogen adsorption isotherm strongly depends on the graphitic character of the surface [8,9]. For the OMC studied, this portion of the isotherm is not affected by pore filling since the filling of the OMC mesopores occurs at higher pressures after the nitrogen monolayer has been formed [3]. Furthermore, the external surface of the OMC is small as compared to the mesopore surface. The shape of the low-pressure isotherm therefore essentially depends on the graphitic character of the mesopore surface. Accordingly, by analysis of the low-pressure adsorption data information on the graphitic character of the mesopore surface can be obtained.

*Corresponding author. Tel.: +1-418-656-2131x6931; fax: +1-418-656-2091.

E-mail addresses: hans.darmstadt@gch.ulaval.ca (H. Darmstadt), rryoo@mail.kaist.ac.kr (R. Ryoo).

0008-6223/02/$ – see front matter
PII: S0008-6223(02)00187-2

The comparison of the surface spectroscopy and gas adsorption results allows one to estimate how representative the surface spectroscopic results are for the entire surface of the OMC. The OMC were produced in MCM-48 and SBA-15 silica matrices, respectively, at different pyrolysis and post-pyrolysis heat treatment temperatures. An important difference between the two matrices is that in the case of SBA-15 the OMC are a replica of the matrix, whereas the structure of OMC produced in MCM-48 changes upon removal of the matrix [10].

2. Experimental procedure

2.1. Materials

The OMC were produced by pyrolysis of sucrose impregnated into a MCM-48 and a SBA-15 silica matrix, respectively. Different pyrolysis experiments were performed at temperatures ranging from 700 to 1100 °C. Then, the OMC were liberated by dissolving the silica matrix in either hydrofluoric acid or sodium hydroxide solution. Some samples were subsequently heat treated at temperatures ranging from 1100 to 1600 °C. The synthesis conditions of the mesoporous carbons are summarised in Table 1. Detailed information on the synthesis of the MCM-48 [11] and the SBA-15 [10] silica matrices, as well as on the synthesis of the OMC [10,12], has already been published. The XRD patterns were recorded on a Rigaku D/MAX-III diffractometer using Cu Kα radiation.

2.2. X-ray photoelectron spectroscopy (XPS)

An ESCALAB MK II spectrometer (VG Scientific, East Grinstead, UK) equipped with a Microlab system from Vacuum Generators (Hastings, UK) with non-monochromatized Mg Kα radiation was used for the XPS experiments. The binding energy scale was corrected by referring to the C_1 peak in the C_{1s} signal at 284.4 eV. However, the corrections made were smaller than 0.05 eV. The pressure during the experiments was lower than 10^{-9} mbar. After removal of satellites and of a non-linear background from the spectra, a mixed Gaussian–Lorentzian product function was used to describe the shape of the peaks [13]:

$$I = \frac{I_0}{\left(1 + \frac{m(x - x_0)^2}{b^2}\right) \exp\left(\frac{(1 - m)\ln 2(x - x_0)^2}{b^2}\right)} \quad (1)$$

where I is the intensity, I_0 is the maximum peak height, x is the binding energy, x_0 is the binding energy at the peak centre, b is a parameter for the peak width that is nearly half the full width at half maximum (FWHM) and m is the Gauss–Lorentz mixing ratio; with $m = 0$ a pure Gaussian curve is obtained, whereas $m = 1$ gives a pure Lorentzian curve. The C_1 peaks of the carbon spectra had an asymmetric shape. Their shape was described by an exponential tail, added to the high binding energy side of the peak [13]:

$$I' = I + (1 - I)(1 - \mathrm{TMR})\, e^{-\mathrm{ETR}(x - x_0)} \quad (2)$$

where I' is the intensity of the asymmetric peak, TMR is the tail mixing ratio and ETR is the exponential tail ratio. A program developed at Université Laval was used to calculate the relative sensitivity factors for the determination of the elemental composition on the surface. This program considers the Scofield photo-ionisation cross-sec-

Table 1
Synthesis parameters of the ordered mesoporous carbons

MCM-48 matrix				SBA-15 matrix			
Sample	Temperature [°C]		Solvent for the matrix	Sample	Temperature [°C]		Solvent for the matrix
	pyrolysis	post-pyrolysis heat-treatment			pyrolysis	post-pyrolysis heat-treatment	
CMK-1F(A)	700	–	HF	CMK-3F(A)	700	–	HF
CMK-1F(B)	900	–	HF	CMK-3F(B)	900	–	HF
CMK-1F(C)	900	1100[a]	HF	CMK-3F(C)	900	1100[a]	HF
CMK-1F(D)	1100	–	HF	CMK-3F(D)	900	1300[b]	HF
CMK-1F(E)	900	1300[b]	HF	CMK-3F(E)	900	1600[b]	HF
CMK-1F(F)	900	1600[b]	HF				
CMK-1Na(A)	700	–	NaOH	CMK-3Na(A)	700	–	NaOH
CMK-1Na(B)	900	–	NaOH	CMK-3Na(B)	900	–	NaOH
CMK-1Na(C)	900	1100[a]	NaOH	CMK-3Na(C)	1100	–	NaOH
CMK-1Na(D)	900	1300[b]	NaOH				
CMK-1Na(E)	900	1600[b]	NaOH				

[a] Under vacuum.
[b] Under nitrogen.

tions, angular asymmetry factors, transmissions and the electron mean free path in the calculation. The program assumes that no concentration gradient exists in the volume probed. The surface area probed by XPS was approximately 5 mm^2.

2.3. Secondary ion mass spectroscopy (SIMS)

A Vacuum Generator SIMSLAB equipped with a Wien-filtered AG61 ionisation ion gun and an MM12-12S quadrupole mass spectrometer was used for the SIMS experiments. The SIMS spectra were recorded using Ar^+ ions with a current density smaller than 1 nA/cm^2 and an energy of 1 keV at a pressure lower than 10^{-7} Pa. The total ion dose after recording the positive and negative SIMS spectra at these settings was lower than $0.5 \cdot 10^{13}$ ions/cm^2. It was shown previously that below an ion dose of $1.0 \cdot 10^{13}$ ions/cm^2 no significant degradation of carbonaceous surfaces takes place [14]. Thus, in the present work true static SIMS spectra were obtained. The argon ion beam diameter was 100 μm, the scanned surface area was 16 mm^2 and the angles of incidence and emission were 45 and 0° with respect to the surface normal, respectively. The mass resolution was better than 0.6 atomic mass units (amu) at 5% peak height. The powdered OMC were placed in stainless steel sample holders where they were only held by gravity.

3. Results and discussion

3.1. Surface composition determined by XPS

The survey spectra of the OMC showed in addition to peaks of carbon and oxygen only small signals of silicon and fluorine. As an example, the survey spectrum of sample CMK-1F(C) is presented in Fig. 1. On the OMC liberated from the silica matrix with sodium hydroxide solution (series CMK-1Na and CMK-3Na) no sodium was found. Fluorine was only detected on samples liberated by dissolving the silica matrix in hydrofluoric acid (series CMK-1F and CMK-3F), indicating that the fluorine originated from the hydrofluoric acid. It should be recalled that hydrogen, which is most probably present on the carbon surface, cannot be detected by XPS.

The most important element on the surface was carbon, as expected. Its concentration ranged from 93.6 to 100.0 atom % (Table 2). With increasing pyrolysis or post-pyrolysis heat treatment temperature, the surface concentration of non-carbon elements decreased. This decrease can be explained by removal of thermally unstable surface functional groups (e.g. –OH and –COOH). On the surface of one of the samples heat treated at 1600 °C (CMK-3F(E)) no elements other than carbon were found.

The low oxygen concentration on the surface of the heat-treated OMC is an indication that the surface of these

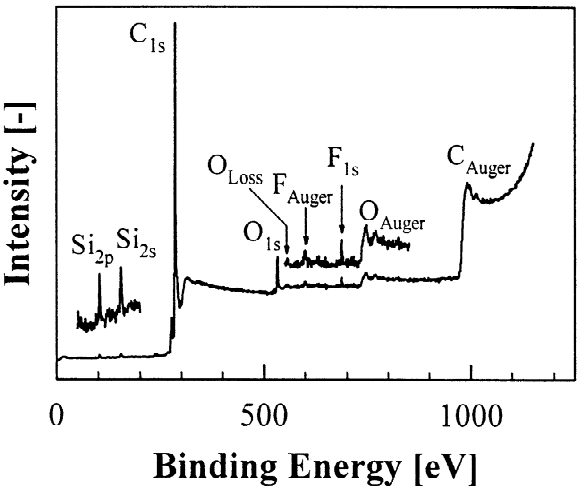

Fig. 1. XPS Survey spectrum, sample CMK-1F(C).

samples was well ordered with no or only a very small concentration of defects. This becomes evident by comparison with other carbonaceous solids. For activated carbons, it was observed that an important portion of the oxygen lost upon heat treatment was re-adsorbed as soon as the heat-treated activated carbon came in contact with the atmosphere [15]. It was assumed that surface defects were created during removal of the oxygen. These defects did not 'heal' during the heat treatment and acted as 'active' sites for the re-adsorption of oxygen. In the present investigation, the heat treated OMC were in contact with

Table 2
Elemental surface composition

Sample	Element [atom %]			
	C	O	Si	F
CMK-1F(A)	95.4	4.1	0.2	0.3
CMK-1F(B)	96.3	2.9	0.3	0.5
CMK-1F(C)	93.6	4.6	1.1	0.7
CMK-1F(D)	94.2	4.4	0.6	0.8
CMK-1F(E)	99.0	0.7	0.3	[a]
CMK-1F(F)	99.1	0.8	0.1	[a]
CMK-1Na(A)	94.8	5.2	[a]	[a]
CMK-1Na(B)	95.8	4.2	0.2	[a]
CMK-1Na(C)	95.4	3.4	1.2	[a]
CMK-1Na(D)	97.5	1.5	1.0	[a]
CMK-1Na(E)	99.7	0.3	[a]	[a]
CMK-3F(A)	96.5	3.5	[a]	[a]
CMK-3F(B)	97.0	2.4	0.3	0.3
CMK-3F(C)	98.2	1.5	0.3	[a]
CMK-3F(D)	99.2	0.7	0.1	[a]
CMK-3F(E)	100.0	[a]	[a]	[a]
CMK-3Na(A)	95.9	4.1	[a]	[a]
CMK-3Na(B)	96.8	2.9	0.3	[a]
CMK-3Na(C)	97.1	2.5	0.4	[a]

[a] Below the detection limit at reasonable acquisition time.

the atmosphere for a considerable period of time prior to the spectroscopic characterisation. The low surface oxygen concentration on the heat-treated OMC indicates, therefore, that there was only a small concentration of defects on the surface of the heat-treated samples, which could react with atmospheric oxygen.

3.2. XPS silicon spectra

The silicon detail spectra were recorded for two OMC (samples CMK-1F(B) and CMK-1F(C)). These spectra showed a doublet with a binding energy (BE) of approximately 102.7 eV for the $2p_{3/2}$ peak (Fig. 2). This BE is typical for silicon atoms in silicates and silica [16]. The BE of silicon atoms with bonds to carbon atoms is considerably lower (101.0 eV, [16]) and no indication for a peak at this BE was found in the spectra. It can therefore be concluded that small quantities of non-dissolved silica were left on the surface of the samples, regardless if the dissolution was performed with hydrofluoric acid or with sodium hydroxide.

3.3. XPS fluorine spectra

On the surface of some OMC, liberated from the matrix by hydrofluoric acid, fluorine was found. The fluorine spectra showed a peak with a BE of approximately 687.0 eV (Fig. 3). Peaks with such a BE were also observed in the spectra of fluorinated carbon blacks [17]. The BE of inorganic fluorides is considerably lower (~684.0 eV) [16]. It seems, therefore, likely that during dissolution of the silica framework with hydrofluoric acid, carbon–fluorine groups were formed on the surface of some OMC. Surface fluorine concentrations of up to 0.8 atom % were found (Table 2). The quantification of elements in such a small concentration by XPS contains some experimental uncertainty. However, even when this is taken into account, the surface fluorine concentration on the OMC seems to depend on the silica matrix used for their synthesis. The OMC formed in MCM-48 contained more fluorine on the surface as compared to samples formed in SBA-15.

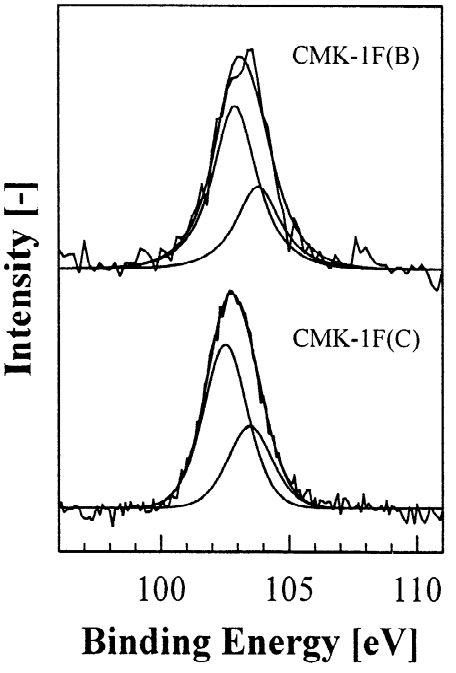

Fig. 2. XPS Silicon 2p spectra, samples CMK-1F(B) and CMK-1F(C); normalised to the same height.

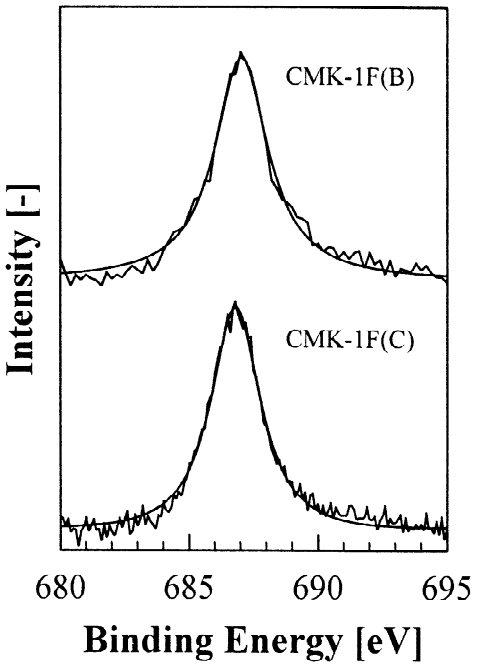

Fig. 3. XPS Fluorine 1s spectra, samples CMK-1F(B) and CMK-1F(C); normalised to the same height.

3.4. XPS oxygen spectra

The oxygen spectra were fitted to four peaks (Fig. 4): a peak for oxygen atoms with two bonds to carbon atoms (O_1, C=O, BE = 531.1 eV), a peak for oxygen atoms with one bond to a carbon atom (O_2, C–OH, BE = 532.8 eV) and to two peaks which could be due to adsorbed water and oxygen, respectively (O_3 and O_4, BE = 535.1 and 537.6 eV) [18,19].

As mentioned above, the silicon spectra indicated the presence of non-dissolved silicates on the carbon OMC. The BE of oxygen atoms in silicates is approximately 532.0 eV [20]. These oxygen atoms will therefore contribute to the O_2 peak. This contribution can be estimated by

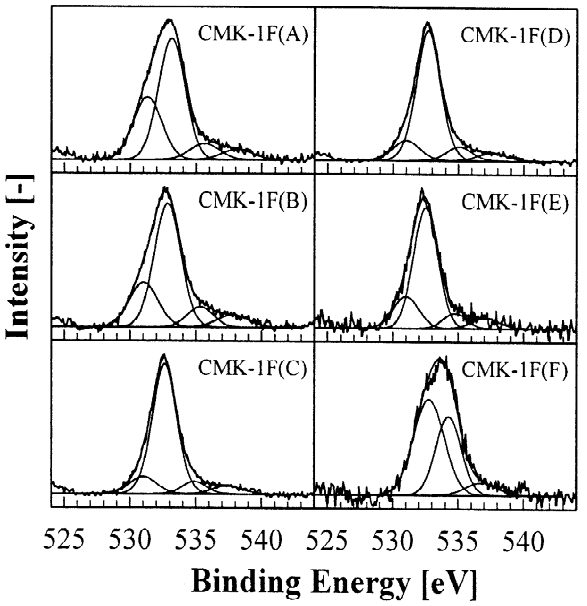

Fig. 4. XPS oxygen 1s spectra, samples CMK-1F(A) to CMK-1F(F); normalised to the same height.

calculating the oxygen concentration in silica. Assuming that all silicon atoms are present in silica (no organic silicon compounds, as confirmed by the silicon spectra) and that all silicon atoms are bonded to two oxygen atoms the concentration of oxygen in silica is two times the concentration of silicon:

$$O_{silica} = 2 \cdot Si_{total} \quad (4)$$

where O_{silica} is the concentration of oxygen in silica and Si_{total} is the total concentration of silicon (Table 2). In order to obtain the contribution of 'C–OH type' oxygen, the area corresponding to these oxygen atoms is then subtracted from the O_2 peak:

$$A(O_2, C{-}OH) \sim A(O_2, C{-}OH + SiO_2) - \frac{O_{silica}}{O_{total}} \quad (5)$$

where $A(O_2, C–OH)$ is the relative area of the O_2 peak due to C–OH groups, $A(O_2, C–OH + SiO_2)$ is the relative area of the O_2 peak (Table 3) and O_{total} is the total concentration of oxygen (Table 2). It should be mentioned that because of the low surface concentrations of silicon this estimation is a relatively rough approximation.

In all oxygen spectra the O_2 peak was more intense than the O_1 peak. This was also the case when the contribution of oxygen atoms in silicates was subtracted from the O_2 peak (Table 3). These data indicate that the surface concentration of C–OH type oxygen was higher than the concentration of C=O type oxygen.

3.5. XPS carbon spectra

The carbon spectra were fitted to six peaks: a peak for

Table 3
XPS oxygen spectra, peak area

Sample	Relative peak area [%]				
	O_1	O_2	O_2[a]	O_3	O_4
	C=O	C–OH, Si–O	C–OH	$H_2O_{ads}/O_{2\,ads}$	
CMK-1F(A)	31	56	46	8	5
CMK-1F(B)	23	61	41	9	7
CMK-1F(C)	11	75	28	7	5
CMK-1F(D)	13	74	46	8	6
CMK-1F(E)	18	68	–	8	6
CMK-1F(F)	–	55	30	37	7
CMK-1Na(A)	32	57	57	8	5
CMK-1Na(B)	22	63	44	9	6
CMK-1Na(C)	–	72	2	10	2
CMK-1Na(D)	–	71	–	22	7
CMK-1Na(E)	5	76	76	16	3
CMK-3F(A)	30	57	57	8	5
CMK-3F(B)	19	66	41	9	7
CMK-3F(C)	14	71	31	6	9
CMK-3F(D)	15	66	38	14	5
CMK-3F(E)	–	–	–	–	–
CMK-3Na(A)	34	52	52	7	7
CMK-3Na(B)	20	64	44	9	7
CMK-3Na(C)	19	65	33	9	7

[a] Estimated area of the O_2 peak due to oxygen atoms with one bond to carbon, Eq. (5).

carbon atoms with bonds to carbon and/or hydrogen atoms (C_1, BE = 284.4 eV [18,21]); to three peaks for carbon atoms with one, two and three bonds to oxygen atoms (C_2, C_3, C_4; C–OH, C=O, COOH, BE = 285.9, 287.4 and 288.9 eV [18,21]) and to two $\pi \rightarrow \pi^*$ peaks (C_5, C_6, BE = 290.4 and 294.4 eV, [22]). The C_3 peak also contains a contribution from carbon atoms with one bond to fluorine [17]. The full width at half maximum (FWHM) of the C_1 peak was 1.0–1.2 eV, 2.0±0.2 eV for the C_2–C_4 peaks and 3.3 eV±0.2 eV for the C_5 and C_6 peaks. The C_1 peak had an asymmetrical shape, whereas the other peaks were symmetrical (Figs. 5a and 5b).

The asymmetry of the C_1 peak obtained by the fitting routine is strongly correlated to the areas of the peaks assigned to carbon–oxygen and carbon–fluorine groups (C_2–C_4). The concentration of these groups depends of course on the surface concentration of oxygen and fluorine. It is therefore possible to add the following constraint to the fitting procedure, which links the area of these peaks to the surface concentration of organic oxygen and fluorine:

$$\frac{\text{Area } C_2 \text{ peak} + \text{Area } C_3 \text{ peak} + 2 \cdot \text{Area } C_4 \text{ peak}}{\text{Total area of the carbon signal}} = \frac{\text{Conc. oxygen} + \text{Conc. fluorine}}{\text{Conc. carbon}} \quad (3)$$

The area of the C_4 peak is multiplied by a factor of two because this peak was assigned to –COOH groups, where one carbon atom is bonded to two oxygen atoms. Since the escape depths of carbon, oxygen and fluorine are different, it has to be assumed that no concentration gradient exists in the volume probed by XPS. The same assumption was made for the calculation of the elemental composition.

All carbon spectra were dominated by an intense, asymmetrical C_1 and a smaller $\pi \rightarrow \pi^*$ (C_5) peak. Such spectra are typical for carbonaceous samples with a graphite-like, polyaromatic surface such as carbon blacks [23] and carbon fibres [18,21]. There were small, but significant differences between the carbon spectra. Important information on the polyaromatic character of a carbon surface can be obtained from different peak parameters [24]. With increasing polyaromatic character, the relative area of the $\pi \rightarrow \pi^*$ peak (C_5) increases [25], the C_1 peak becomes more asymmetrical [26] and its FWHM decreases [27]. In the present work, all these parameters were used to describe the polyaromatic character of the OMC surface. The determination of the area of the $\pi \rightarrow \pi^*$ peak and the FWHM of the C_1 peak is straightforward, whereas there are several possibilities to describe the asymmetry of the C_1 peak [21]. In the present work, the asymmetry of this peak was described by the ratio of the peak area on the high and low binding energy side of the peak maximum (A_H/A_L). A symmetrical peak has an A_H/A_L value of 1, whereas asymmetrical peaks have larger A_H/A_L values. The treatment temperature had a pronounced effect on the carbon spectra. For the samples of the CMK-1F series it can easily be seen that the area of the $\pi \rightarrow \pi^*$ peak increased with increasing heat treatment temperature (Figs. 5a and 5b and Table 4). Furthermore, the C_1 peak became narrower and its asymmetry increased (Table 4, not easy to see in Figs. 5a and 5b). All these

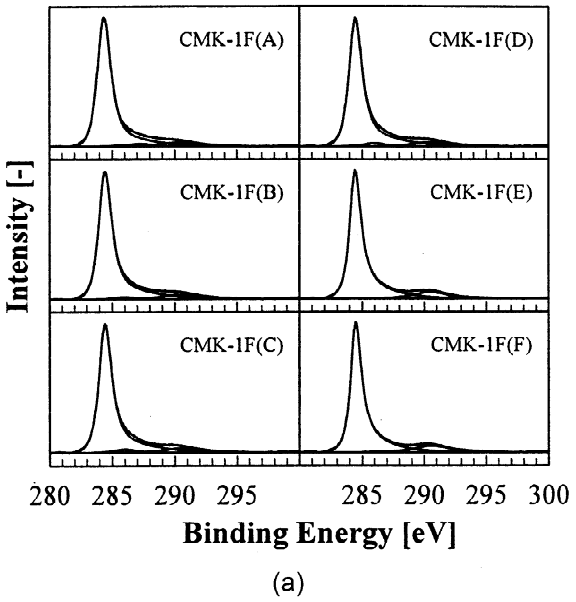

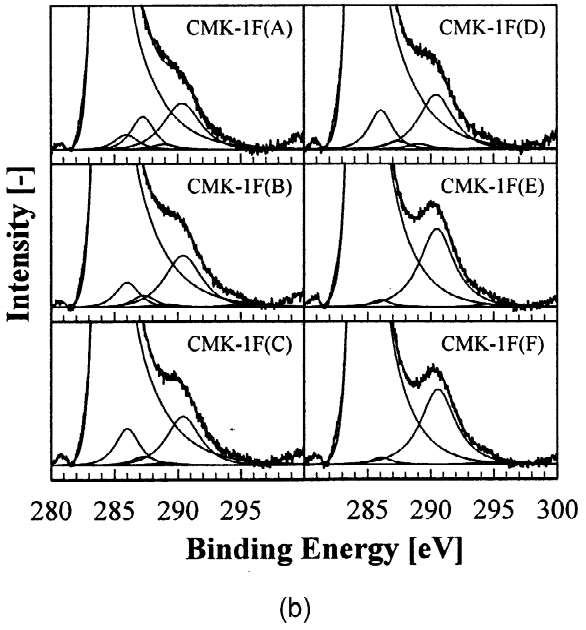

Fig. 5. (a) XPS carbon 1s spectra, samples CMK-1F(A) to CMK-1F(F); normalised to the same height; (b) XPS carbon 1s spectra, samples CMK-1F(A) to CMK-1F(F); enlarged to 10% of maximum height.

Table 4
XPS carbon spectra; peak area and fit parameter of the C_1 peak

Sample	Relative peak area [%]						Parameter of the C_1 peak	
	C_1 C–C	C_2 C–OH	C_3 C=O	C_4 COOH	C_5 $\pi\rightarrow\pi^*$	C_6 $\pi\rightarrow\pi^*$	Asymmetry[a] A_H/A_L	FWHM [eV]
CMK-1F(A)	89.3	1.3	2.8	0.4	6.2	0.0	1.64	1.23
CMK-1F(B)	89.2	2.2	1.0	0.3	7.2	0.2	1.72	1.18
CMK-1F(C)	89.5	3.3	0.8	0.2	6.2	0.0	1.72	1.15
CMK-1F(D)	88.4	3.3	0.7	0.5	7.0	0.1	1.75	1.16
CMK-1F(E)	87.9	0.6	0.0	0.0	11.3	0.2	1.81	1.00
CMK-1F(F)	87.8	0.6	0.0	0.0	11.4	0.2	1.83	0.95
CMK-1Na(A)	87.6	1.9	3.1	0.7	6.6	0.1	1.55	1.23
CMK-1Na(B)	89.5	2.0	1.1	0.4	7.1	0.0	1.59	1.16
CMK-1Na(C)	90.8	1.2	0.0	0.2	7.8	0.0	1.72	1.14
CMK-1Na(D)	90.6	0.6	0.0	0.0	8.5	0.3	1.72	1.05
CMK-1Na(E)	87.2	0.6	0.0	0.0	11.8	0.4	1.75	0.92
CMK-3F(A)	88.8	1.3	2.5	0.3	6.8	0.3	1.66	1.22
CMK-3F(B)	89.2	2.0	0.7	0.1	7.7	0.3	1.74	1.18
CMK-3F(C)	90.5	1.0	0.0	0.0	8.3	0.2	1.72	1.11
CMK-3F(D)	90.0	0.6	0.0	0.0	9.2	0.3	1.79	1.04
CMK-3F(E)	89.2	0.0	0.0	0.0	10.6	0.2	1.75	0.92
CMK-3Na(A)	88.9	1.5	2.5	0.5	6.7	0.0	1.59	1.18
CMK-3Na(B)	89.5	2.0	0.6	0.2	7.2	0.1	1.69	1.17
CMK-3Na(C)	89.5	2.2	0.2	0.0	7.2	0.2	1.55	1.12

[a] Ratio of the peak area on the high and low binding energy side of the peak maximum.

changes indicate an increasing polyaromatic character of the surface with increasing treatment temperature.

Even if the agreement between the three parameters that describe the polyaromatic character of the surface was reasonably good, the usefulness of the parameters was not the same. The three parameters are plotted in Fig. 6 as a function of the highest temperature used during the synthesis of the OMC. The data indicate some scattering for the peak asymmetry (A_H/A_L value) and the area of the $\pi\rightarrow\pi^*$ peak. The FWHM data, on the other hand, gave a much smoother curve, indicating that for the samples studied the FWHM is the most suitable parameter for the description of the polyaromatic character of the OMC surface.

As already mentioned, the OMC were formed in the pore system of a silica matrix. The OMC can be described as a network of interconnected carbon rods. It is evident that the network structure of the carbon rods depends on the pore structure of the silica matrix. The pore structure of the MCM-48 and the SBA-15 silica matrices differs considerably [1,2]. Consequently, there are also large differences between the network structures of the OMC synthesised in the two matrices. In spite of these differences, for a given treatment temperature, the FWHM in the carbon spectra of samples produced in either a MCM-48 and the SBA-15 silica matrix was very similar. This indicates that the determining factor was the treatment temperature, rather than the OMC network structure.

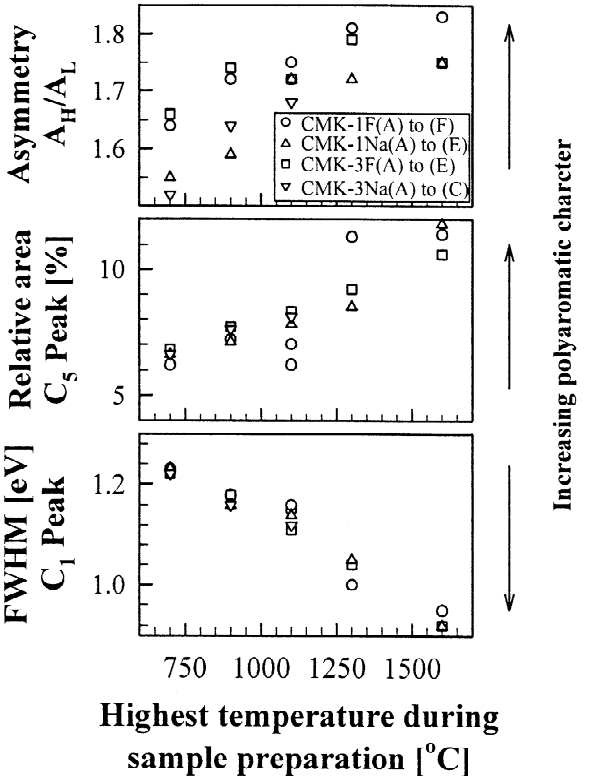

Fig. 6. Polyaromatic character of the surface as a function of the temperature during sample preparation.

3.6. SIMS spectra

Static SIMS was used as a second surface spectroscopic method. In the SIMS experiment the sample surface is bombarded with high-energy ions, causing the ejection of ions and neutral species. Which species are ejected depends on the chemical nature of the sample surface. The SIMS spectra of carbonaceous solids with a polyaromatic surface (e.g. carbon blacks [14] and carbon fibres [28]) show intense peaks of C_2H^- and C_2^- ions. These materials consist of graphene layers. The most important contribution to the C_2H^- peak arises from the edge of graphene layers, whereas most of the C_2^- ions originate from the interior of the graphene layers [14,29]. The ratio of the areas of these two peaks (C_2H^-/C_2^-) is therefore a measure for the inverse size of the graphene layer on the surface of the sample. A low C_2H^-/C_2^- ratio indicates large graphene layers or a high polyaromatic character. This was confirmed by the SIMS spectra of reference compounds. For polycrystalline graphite, the reference compound for a large polyaromatic system, a C_2H^-/C_2^- ratio of 0.25 was found, whereas the spectrum of 3,4-benzofluoranthene, consisting of five condensed aromatic rings, showed a C_2H^-/C_2^- ratio of 2.20 (Table 5).

The SIMS spectra strongly depended on the pyrolysis and the post-pyrolysis heat treatment temperature during synthesis of the OMC. As shown for the series CMK-1Na in Fig. 7, the relative intensity of the C_2H^- peak (and therefore also the C_2H^-/C_2^- ratio) decreased with increasing temperature, indicating an increasing polyaromatic character of the surface. However, this decrease was limited to temperatures below approximately 1100 °C. Heat treatment at higher temperatures only had a very limited effect on the C_2H^-/C_2^- ratio (Fig. 8). This observation indicates that at approximately 1100 °C a 'maximum polyaromatic character' of the outer OMC surface was reached. However, it is also possible that static SIMS fails to differentiate between samples with a very high polyaromatic character. It can be seen in Fig. 7 that for the OMC heat-treated at temperatures above 1100 °C (e.g. samples CMK-1Na(D) and CMK-1Na(E)) the C_2H^- peak was very small. Thus, differences between different samples treated at temperatures above 1100 °C are not easy to detect.

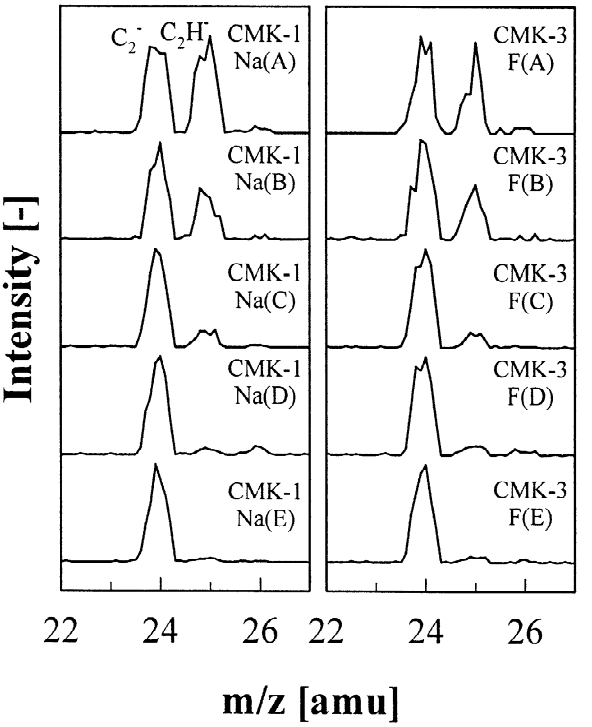

Fig. 7. SIMS spectra, negative ions, series CMK-1Na and CMK-3F; normalised to the same height.

It is interesting to note that the C_2H^-/C_2^- ratios of the samples heat treated above 1100 °C were lower as compared to the polycrystalline graphite and other compounds with a graphite-like surface such as rubber blacks and

Table 5
SIMS; C_2H^-/C_2^- ratio (peak area)

Sample	C_2H^-/C_2^- ratio	Sample	C_2H^-/C_2^- ratio
3,4-benzo-fluoranthene	2.20	CMK-3F(A)	0.70
		CMK-3F(B)	0.51
CMK-1F(A)	1.09	CMK-3F(C)	0.15
CMK-1F(B)	0.65	CMK-3F(D)	0.11
CMK-1F(C)	0.48	CMK-3F(E)	0.07
CMK-1F(D)	0.51	CMK-3Na(A)	0.74
CMK-1F(E)	0.06	CMK-3Na(B)	0.34
CMK-1F(F)	0.11	CMK-3Na(C)	0.24
CMK-1Na(A)	0.95	Rubber carbon black, N539	0.51
CMK-1Na(B)	0.58		
CMK-1Na(C)	0.18	Conductive carbon black, XC-72	0.21
CMK-1Na(D)	0.06		
CMK-1Na(E)	0.04	Graphite	0.25

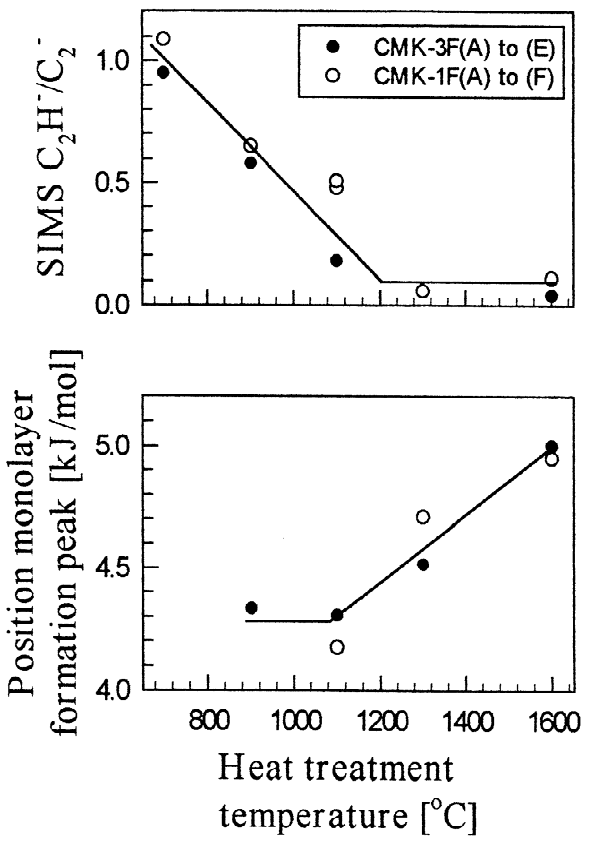

Fig. 8. SIMS C_2H^-/C_2^- ratio (measure for the polyaromatic character of the outer surface) and position of the monolayer formation peak (measure for the order of the mesopore surface) as a function of the heat treatment temperature.

conductive carbon blacks (Table 5). Especially conductive carbon blacks have a high polyaromatic character, which favours their electrical conductivity. This suggests that the outer surface of the heat-treated OMC had an especially high polyaromatic character.

The temperature dependence of the C_2H^-/C_2^- ratio was very similar for the different series of OMC. This confirms the conclusion from the XPS study that the silica matrix had no or only very little influence on the polyaromatic character of the outer surface of the OMC.

3.7. Comparison of surface spectroscopic with nitrogen adsorption results

It was already mentioned that the outer surface (probed by SIMS and XPS) only represents a very small portion of the total surface of the OMC. The largest portion of the surface is present in narrow mesopores. The OMC constructed with very uniform mesopores represent a special case where the information on the graphitic order of the mesopore surface may be obtained from low-pressure nitrogen adsorption data [3], as described below.

On very homogeneous surfaces such as exfoliated graphite, the adsorption potentials of all adsorption sites are very similar so that the same layers of adsorbed nitrogen are formed almost at the same relative pressure. Thus, in the corresponding isotherms steps are observed which correspond to the successive formation of the various nitrogen layers [30]. The nitrogen adsorption isotherms of less homogeneous samples (e.g. graphitized carbon blacks) only show the monolayer formation step at a relative pressure (P/P_0) of approximately 2 to $5\cdot10^{-4}$ [31]. For more heterogeneous samples (e.g. non-graphitized carbon blacks) the monolayer step cannot be observed in the isotherm [9]. However, even for many of these materials a monolayer formation peak can be found in the corresponding adsorption potential distribution (APD). Formally, the APD may be regarded as a derivative of the adsorption isotherm (logarithmic scale of the relative pressure). The position of the monolayer formation peak depends on the graphitic order of the surface. For graphitized carbon blacks the monolayer formation peaks are located at adsorption potentials between 5 and 5.5 kJ/mol [9]. With decreasing graphitic order, the monolayer formation peak is shifted to lower adsorption potentials [31]. The APD of porous carbons show pore filling peaks which interfere with the monolayer formation peak. However, because of the special pore structure of the OMC, this was not the case for the samples studied in the present work [3]. It was therefore possible to obtain information on the graphitic order of their surface from the position of the monolayer formation peak in the APD. Since the mesopore surface is much larger as compared to the outer surface, the position of the monolayer formation peak depends essentially on the graphitic order of the mesopore surface. This allows the comparison of the graphitic order of the mesopore surface (as studied by low-pressure nitrogen adsorption) to the graphitic order of the outer surface (as studied by SIMS) and to the outer surface plus the region near to the outer surface (as studied by XPS).

For the OMC synthesised at 700 °C no monolayer formation peak was observed, indicating a relatively low graphitic order of the surface. A monolayer formation peak at approximately 4.2 kJ/mol was found in the APD of the OMC synthesised at 900 °C. With increasing synthesis or treatment temperatures (especially above 1100 °C), the monolayer peak was shifted to higher adsorption potentials (Fig. 8). This indicates an increasing graphitic order of the mesopore surface over the entire temperature range studied.

As mentioned above, the polyaromatic character of the outer surface plus the region near to the outer surface can be characterised by the FWHM of the C_1 XPS peak. The FWHM decreased with increasing synthesis temperature and this decrease was more pronounced above 1100 °C (Fig. 6). The temperature dependence was consistent with

the shifts of the N_2 adsorption potentials (Fig. 8). Thus, as it was the case for the mesopore surface, the polyaromatic character of the surface studied by XPS increased over the entire temperature range and especially above 1100 °C. The good correlation between the nitrogen adsorption and the XPS results indicates that, at least for the sample studied here, some information on the chemistry of the internal mesopore surface can be drawn from the XPS results. However, these results from N_2 adsorption and XPS show a significant difference from the temperature dependence of the SIMS C_2H^-/C_2^- ratios, which strongly decreased up to a temperature of 1100 °C and changed only little upon further heating (Fig. 8). As discussed above, this suggests that at 1100 °C the first atomic layer of the outer surface had already reached its 'real' or detectable maximum polyaromatic character, whereas the graphitic or polyaromatic character was still being developed at the internal mesopore surface.

3.8. XRD patterns

Due to the mesoscale structural order of the OMC, Bragg diffractions for these materials are observed at small angles. The pronounced peaks in the XRD patterns of representative CMK-1 and CMK-3 samples (prepared by HF washing) indicated a high long-range structural ordering of the bulk of these materials [6]. With increasing treatment temperature, the peaks became smaller, indicating a decrease of the structural order (Fig. 9). However, even after heating to 1600 °C, the XRD patterns still showed prominent peaks suggesting a considerably high degree of structural order of the heat-treated OMC. The OMC washed with NaOH gave similar XRD patterns (not shown). It was outlined above that the order of the external and internal surface increased upon heating. The different temperature dependence for the surface and the bulk order may be related to changes of the OMC network structure upon heating. As already mentioned above, the OMC structure can be described as a system of interconnected carbon rods. Upon heating, the carbon rods shrink [3]. It is reasonable to assume that this shrinkage influenced the OMS bulk order.

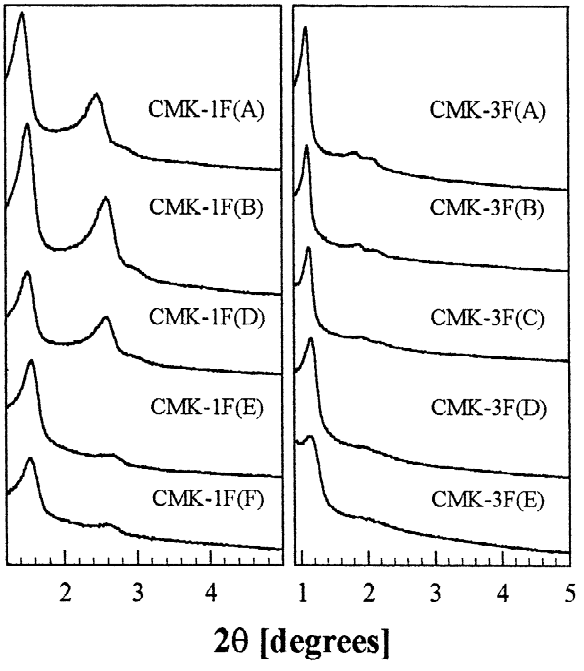

Fig. 9. Powder X-ray diffraction pattern, series CMK-1F and CMK-3F.

4. Conclusions

The outer surface of the ordered mesoporous carbons (OMC) has a graphite-like, polyaromatic character, similar to carbon blacks or carbon fibres. Higher temperatures during pyrolysis or post-pyrolysis heat treatment increase the polyaromatic character considerably. The outer surface of OMC heated to temperatures above 1100 °C has a more pronounced polyaromatic character as compared to polycrystalline graphite, rubber-grade carbon blacks or conductive carbon blacks. Upon heat-treatment, the graphitic character of the mesopore surface also increases.

The structure of the silicate matrix used for the synthesis of the OMC has no influence on the polyaromatic character of the surface. During dissolution of the silicate matrix in hydrofluoric acid, organic fluorine compounds are formed on the surface. A maximum surface fluorine concentration of 0.8 atom % was observed. Furthermore, small concentrations of non-dissolved silicates are present on the surface of the OMC. Dissolution of the silica matrix in sodium hydroxide yields a less contaminated OMC as compared to dissolution in hydrofluoric acid.

Acknowledgements

The authors are thankful to Dr. Alain Adnot for helpful discussion of the surface spectroscopy results and to Dr. Annette Schwerdtfeger for reviewing the manuscript. R. Ryoo gratefully acknowledges that this work was supported in part by the Korean Ministry of Science and Technology through the Creative Research Initiative Program, and by the School of Molecular Science through the Brain Korea 21 Project.

References

[1] Ryoo R, Joo SH, Jun S. Synthesis of highly ordered carbon molecular sieves via template-mediated structural transformation. J Phys Chem B 1999;103:7743–6.

[2] Shin HJ, Ryoo R, Kruk M, Jaroniec M. Modification of SBA-15 pore connectivity by high-temperature calcination investigated by carbon inverse replication. Chem Commun 2001;349:50.
[3] Darmstadt H, Roy C, Kaliaguine S, Choi S, Ryoo R. Pore structure and graphitic surface order of mesoporous carbon molecular sieves by low-pressure nitrogen adsorption. In: Carbon 2001, International Conference on Carbon, Lexington, Kentucky, USA July 14–19, 2001.
[4] Seke MD, Sandenbergh RF, Vegter NM. Effects of the textural and surface properties of activated carbon on the adsorption of gold di-cyanide. Miner Eng 2000;13:527–40.
[5] Wu SH, Pendleton P. Adsorption of anionic surfactant by activated carbon: effect of surface chemistry, ionic strength, and hydrophobicity. J Colloid Interface Sci 2001;243:306–15.
[6] Guo J, Lua AC. Effect of surface chemistry on gas-phase adsorption by activated carbon prepared from oil-palm stone with pre-impregnation. Sep Purif Technol 2000;18:47–55.
[7] Karanfil T, Kitis M, Kilduff JE, Wigton A. Role of granular activated carbon surface chemistry on the adsorption of organic compounds. 2. Natural organic matter. Environ Sci Technol 1999;33:3225–33.
[8] Turner AR, Quirke N. A grand canonical Monte Carlo study of adsorption on graphitic surfaces with defects. Carbon 1998;36:1439–46.
[9] Darmstadt H, Roy C. Comparative investigation of defects on carbon black surfaces by nitrogen adsorption and SIMS. Carbon 2001;39:841–8.
[10] Jun S, Joo SH, Ryoo R, Kruk M, Jaroniec M, Liu Z, Ohsuma T, Terasaki O. Synthesis of new nanoporous carbon with hexagonally ordered mesostructure. J Am Chem Soc 2000;43:10712–3.
[11] Ryoo R, Joo SH, Kim JM. Energetically favored formation of MCM-48 from cationic-neutral surfactant mixtures. J Phys Chem B 1999;103:7435–40.
[12] Kruk M, Jaroniec M, Ryoo R, Joo SH. Characterization of ordered mesoporous carbons synthesized using MCM-48 silicas as templates. J Phys Chem B 2000;104:7960–8.
[13] Sherwood PMA. In: Briggs D, Seah MP, editors, Practical surface analysis by Auger and X-ray photoelectron spectroscopy, Chichester, UK: John Wiley & Sons Ltd, 1983, p. 445.
[14] Darmstadt H, Sümmchen L, Roland U, Roy C, Kaliaguine S, Adnot A. Surface versus bulk chemistry of pyrolytic carbon blacks by SIMS and Raman spectroscopy. Surf Interface Anal 1997;25:245–53.
[15] Menéndez JA, Phillips J, Xia B, Radovic LR. On the modification and characterization of chemical surface properties of activated carbon: in the search of carbons with stable basic properties. Langmuir 1996;12:4404–10.
[16] Wagner CD, Riggs WM, Davis LE, Moulder JF, Muilenberg GE. In: Handbook of X-ray photoelectron spectroscopy, Eden Prairie, MN, USA: Perkin-Elmer Corporation, 1979.
[17] Nanse G, Papirer E, Fioux P, Moguet F, Tressaud A. Fluorination of carbon blacks: an X-ray photoelectron spectroscopy study: I. A literature review of XPS studies of fluorinated carbons. XPS investigation of some reference compounds. Carbon 1997;35:175–94.
[18] Xie Y, Sherwood PMA. X-ray photoelectron spectroscopic studies of carbon fiber surfaces. II. Differences in the surface chemistry and bulk structure of different carbon fibers based on poly(acrylonitrile) and pitch and comparison with various graphite samples. Chem Mater 1990;2:293–8.
[19] Xie Y, Sherwood PMA. X-ray photoelectron-spectroscopic studies of carbon fiber surfaces. Part IX. The effect of microwave plasma treatment on carbon fiber surfaces. Appl Spectrosc 1989;43:1153–8.
[20] Barr TL. In: Modern ESCA: the principles and practice of X-ray photoelectron spectroscopy, Boca Raton, FL, USA: CRC Press, 1984, p. 283.
[21] Desimoni E, Casella GI, Morone A, Salvi AM. XPS determination of oxygen-containing functional groups on carbon-fibre surfaces and the cleaning of these surfaces. Surf Interface Anal 1990;15:627–34.
[22] Gardella JA, Ferguxson SA, Chin RL. pi*→pi shakeup satellites for the analysis of structure and bonding in aromatic polymers by X-ray photoelectron spectroscopy. Appl Spectrosc 1986;40:224–32.
[23] Darmstadt H, Roy C, Kaliaguine S. ESCA characterization of commercial carbon blacks and of carbon blacks from vacuum pyrolysis of used tires. Carbon 1994;32:1399–406.
[24] Barr TL, Yin M. Concerted X-ray photoelectron spectroscopy study of the character of select carbonaceous materials. J Vac Sci Technol A 1992;10:2788–95.
[25] Kelemen SR, Rose KD, Kwiatek PJ. Carbon aromaticity based on XPS Π to Π* signal intensity. Appl Surf Sci 1992;64:167–73.
[26] Cheung TTP. X-ray photoemission of polynuclear aromatic carbon. J Appl Phys 1984;55:1388–93.
[27] Morita K, Murata A, Ishitani A, Muragana K, Ono T, Nakajima A. Characterization of commercially available PAN (polyacrylonitrile)-based carbon fibers. Pure Appl Chem 1986;58:456–68.
[28] Darmstadt H, Roy C, Kaliaguine S, Ting J-M, Alig RL. Surface spectroscopic analysis of vapour grown carbon fibres prepared under various conditions. Carbon 1998;36:1183–90.
[29] Albers P, Deller K, Despeyroux BM, Prescher G, Schäfer A, Seibold K. SIMS/XPS investigations on activated carbon catalyst supports. J Catal 1994;150:368–75.
[30] Thomy A, Duval X. Stepwise isotherms and phase transitions in physisorbed films. Surf Sci 1994;299–300:415–25.
[31] Kruk M, Li ZJ, Jaroniec M, Betz WR. Nitrogen adsorption study of surface properties of graphitized carbon blacks. Langmuir 1999;15:1435–41.